

Pressure induced Topological Dirac semimetals in XCdP(X=Na, K)

Shivendra Kumar Gupta,^{1,*} Nikhilesh Singh,¹ Saurabh Kumar Sen,¹ and Poorva Singh^{1,†}

¹*Department of Physics,
Visvesvaraya National Institute of Technology, Nagpur, 440010, India*
(Dated: December 12, 2023)

We present a theoretical investigation on the pressure-induced emergence of Dirac semimetallic properties in the XCdP (X = Na, K) materials, employing first-principles calculations. Dirac semimetals, characterized by linear dispersion relations in their electronic band structures, have gained prominence due to their unique topological features and potential applications in electronic devices. Through systematic calculations, we explore the electronic structure evolution of NaCdP and KCdP under varying pressure conditions. Our findings reveal a compelling transition to a Dirac semimetallic state in both NaCdP and KCdP under applied pressure. The electronic band structures exhibit distinct Dirac cones at the Fermi level, indicating the presence of massless Dirac fermions. Moreover, the pressure-induced Dirac semi-metallic phase in these compounds are found to be robust, and are protected by crystal symmetry. We provide a comprehensive analysis of the bandgap, Fermi surface, and other relevant electronic properties, offering insights into the pressure-driven phase transition in NaCdP and KCdP. The tunability of these materials under external pressure suggests their potential utility in next-generation electronic devices and quantum technologies.

I. INTRODUCTION

Topological materials showcase unique properties like dissipationless spin transport through topological-protected surface states[1]. The first topological material discovered was a topological insulator that showed dissipationless spin transport along with the exchange of orbital band characteristic of conduction and valence bands with a small finite bulk band gap[2–4]. Later similar kind of surface properties were also found in the semi-metals exhibiting closing of gap through bulk bands[5]. These kind of semi-metals generated much interest due to their unique properties and were mainly categorized into Dirac semi-metal, Weyl semi-metal, and nodal line and nodal surface semi-metals[6]. Dirac semi-metals have four-fold degenerate zero-dimensional nodal points having linear dispersion in band crossing distinct to Weyl semi-metals which possess two-fold degenerate zero-dimensional nodal points while nodal line or nodal surface semi-metals have either four or two-fold degenerate one-dimensional nodal line or ring or two-dimensional nodal plane[7].

In the last two decades, the development of new topological materials and their classification has provided a path to understand their nature, however, there are some topological classes that need increased attention due to lack of materials realization in experimental framework. One of these types is topological Dirac semi-metal, a type of topological semi-metal (TSM), which is identified by the crossing of conduction and valence bands at discrete points near the Fermi level in the Brillouin zone and linear dispersion relation in all directions [8]. Two Weyl points of opposite chirality overlap to form a 3D massless Dirac point which is sensitive to perturbations. Dirac

semi-metals retain time reversal and inversion symmetries, showcasing unique properties such as giant diamagnetism, quantum magnetoresistance (MR) in the bulk, higher carrier mobility, oscillating quantum spin Hall effect, and the presence of Fermi arcs or Dirac points on the surface. Moreover, by breaking different symmetries, a topological Dirac semi-metal (TDSM) can be converted into other exotic phases such as topological insulators, Weyl semimetals, axion insulators, and topological superconductors [9, 10]. These properties along with the study of related topological quantum phase transitions makes DSMs ideal candidates to investigate.

There are three pre-requisites for a material to be Dirac semimetal. The first and foremost is the four-fold essential degeneracy enforced by nonsymmorphic symmetry at a high symmetry point in the Brillouin zone. BiO_2 and $BiZnSiO_4$ are such materials that come under this category [11]. Secondly, emergence of the accidental Dirac nodes at critical points of topological phase transition in special topological insulator materials having large Rashba splitting, Weyl semimetals, nodal line semimetals, and triple point semimetals. 3D Dirac fermions can be observed at a single quantum critical point as it do not carry a Chern number, however, it requires extreme fine tuning of alloy composition, which limits it to be introduced experimentally[12]. There is also an accidental band crossing DSM, induced by band inversion which is protected by proper axial rotational symmetry, making it quite robust within a finite range of Hamiltonian parameters. Na_3Bi and Cd_3As_2 are such materials that have been confirmed experimentally as topological Dirac semi-metals under this category[13]. Additionally, Dirac semimetals are classified into type I, type II, and type III, based upon the tilting of the band resulting in obeying or breaking of Lorentz invariance. Type I Dirac semimetals exhibit negative magnetoresistance across all directions while obeying Lorentz invariance—a feature found in high-energy physics. This DSM phase has been

* shivendrakumarg900@gmail.com

† poorvasingh@phy.vnit.ac.in

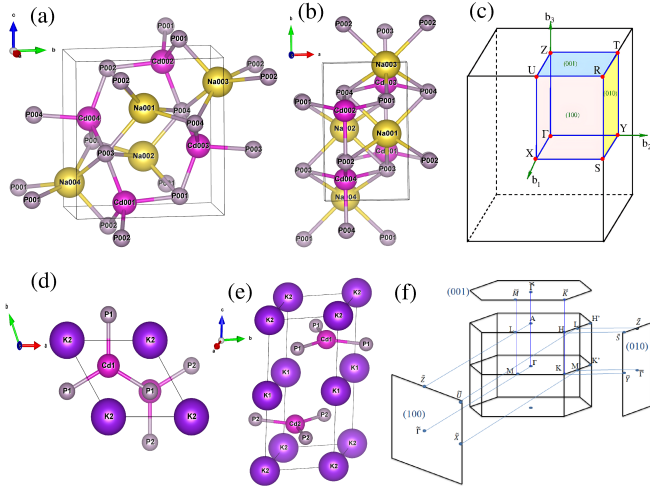


FIG. 1. (a) Crystal structure of NaCdP (b) Crystal structure of NaCdP from different angles. (c) Bulk and surface Brillouin zone [(100),(010),(001)] of orthorhombic crystal structure with different colors. (d) Crystal structure of KCdP (e) Crystal structure of KCdP from different angles. (f) Bulk and surface Brillouin zone [(100),(010),(001)] of hexagonal crystal structure for KCdP.

identified in a variety of crystal structures [10, 14–17]. Type II Dirac semi-metals are characterized by crossing of topologically protected and strongly tilted bands creating electron and hole-like pockets along with breaking of the Lorentz invariance. Type II DSM is proposed as a platform for topological superconductivity and Majorana fermions and is reported in $PtSe_2$ [18], $RbMgBi$ [19], VAL_3 [20], and YPd_2Sn [21] classes. On the other hand type III Dirac semi-metals, also called critical Dirac semi-metals, result from topologically protected tilted bands but have line-like Fermi surfaces with topological invariant $N_2 = 1$ and are theoretically predicted in $Zn_2In_2S_5$ [22], $Hf_xZr_{1-x}Te_2$ [23] and $Ni_3In_2X_2$ ($X = S, Se$)[24].

In order to induce band overlap within the bulk band structure, emergence of topological behaviour typically requires a substantial perturbation. Spin-orbit coupling (SOC) commonly fulfills this criterion. Nevertheless, there exist alternative methods for achieving band crossings. Application of pressure can modify atomic orbital hybridizations or the strength of spin-orbit coupling, thereby leading to band inversion near the Fermi level and facilitating attractive topological phase transitions (TPTs) [25]. This pressure-induced shift in bands can manifest in either unidirectional or multidimensional manners, depending on the specific crystal's demands. Several semi-metals, including LaAs[26], LaSb[27], TmSb[28], TaAs [29], and YbAs[30], have been demonstrated to transition into topologically non-trivial phases under pressure. Furthermore, topological phases in materials like LaSb[31] and SnTe[32] have been observed when subjected to epitaxial strain, and these observations have been experimentally confirmed through angle-resolved photoemission spectroscopy (ARPES) in

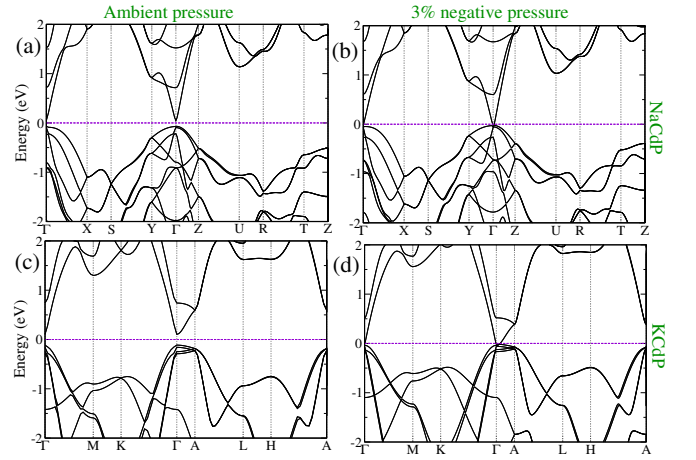


FIG. 2. Electronic bulk band structure including the spin-orbital coupling of (a) NaCdP with ambient pressure (b) NaCdP with c-axis negative uniaxial pressure of 3%. Electronic bulk band structure including the spin-orbital coupling of (c) KCdP with ambient pressure (d) KCdP with all-axis negative triaxial pressure of 3%.

the case of SnTe[32]. In this paper, we have taken computationally predicted n-type thermoelectric materials[33] NaCdP and KCdP which have different crystal structures with finite bulk band gaps of 116meV and 220meV, respectively. Applying suitable pressure allowed the band to shift and overlap at the Γ point resulting in topological phase transition from normal to Dirac semi-metal which is confirmed by the surface band calculation. Analysis of the electronic band structures of NaCdP and KCdP reveals that the DSM phase in these materials is induced by band inversion and is protected by crystal symmetry.

S. No.	Material	Structure	0% pressure	3% pressure
1	NaCdP	Orthorhombic	a=4.38Å b=7.43Å c=7.89 Å	a=4.38Å b=7.43Å c=8.13Å
2	KCdP	Hexagonal	a=4.44Å b=4.44Å c= 10.18Å	a=4.57Å b=4.57Å c= 10.48Å

TABLE I. Optimized lattice parameter of XCdP ($X=Na, K$) for both ambient and strain state.

II. RESULT AND DISCUSSION

First-principles calculation has been done for n-type thermoelectric materials XCdP ($X=Na, K$). The three-dimensional material NaCdP belongs to space group Pnma (62) with an orthorhombic crystal structure with optimized lattice parameters $a= 4.38$, $b=7.43$, and $c=7.89$, as shown in figure 1(a) and 1(b) with different views. The three-dimensional Brillouin zone and corresponding two-dimensional Brillouin zone for NaCdP

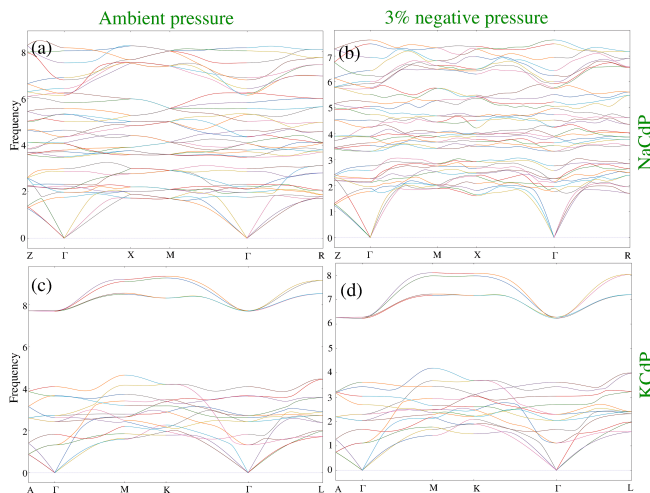


FIG. 3. phonon band structure of (a) NaCdP with ambient pressure. (b) NaCdP with *c*-axis negative uniaxial pressure of 3% (c) phonon band structure of (c) KCdP with ambient pressure. (d) KCdP with all-axis negative triaxial pressure of 3%

are shown with different colors in Figure 1(c). On the other hand, KCdP belongs to the space group $P6_3/mmc$ (194) and has a hexagonal crystal structure with optimized lattice parameters $a=4.44$, $c=10.18$, as shown in Figure 1(d) and 1(e). The three-dimensional Brillouin zone and corresponding two-dimensional Brillouin zone for KCdP are shown in Figure 1(f). The absence of imaginary phonon frequency as evident from the phonon bandstructure of NaCdP and KCdP shown in Figures 3(a) and 3(c), ensures the stability of the materials. In the search for topological material, the electronic properties of XCdP at ambient pressure have been calculated and the band structure of XCdP ($X=Na, K$) considering the spin-orbital coupling has been shown in Figure 2(a) and 2(c), respectively. In XCdP the nature of the band is semi-metallic and one of the conduction bands shows a cone-like structure at the Γ point. The NaCdP material features a direct band gap of 116 meV, while KCdP exhibits a larger direct band gap of 220 meV.

With intent to observe the topological phase transition in the material, negative uniaxial pressure has been applied to the *c*-axis of NaCdP. The negative uniaxial pressure allows Volume Expansive Pressure (VEP) in the system in the uniaxial direction and the topological phase transition (TPT) in NaCdP occurs when the lattice constant *c* is increased by 3%, shown in Figure 2(b). The KCdP on the other hand shows topological phase transition at negative triaxial pressure i.e. lattice constant increased by 3%, in all three directions as shown in Figure 2(d). VEP can be experimentally observed in phenomena like cavitation pressure [34]. Phonon dispersion calculations were performed to check the lattice dynamical stability of the proposed crystal systems, NaCdP and KCdP in the strained state, as shown in Figure 3(b) and 3(d), respectively. Phonon studies indicate the practical

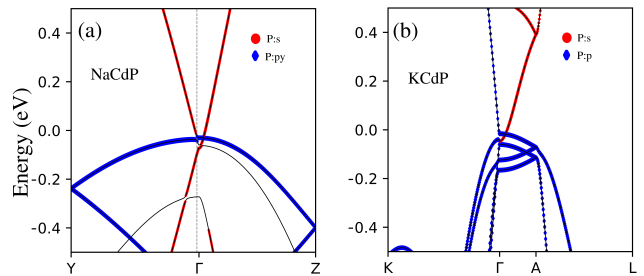


FIG. 4. Band inversion induced Dirac semi-metal (a) NaCdP: band inversion between *s*-orbital and p_y -orbital of P and (b) KCdP: band inversion between *s*-orbital and *p*-orbital of P

feasibility of synthesizing the materials. For the current study, phonon dispersion curves are obtained at ambient pressure as well as at negative uniaxial pressure (3% VEP) with no imaginary frequencies showing that these are dynamically stable in nature.

In strained states, the semi-metallic nature of materials is evident through the crossing in the bulk band. The linear crossing of doubly-degenerate bands signifies the topological Dirac semimetal (TDSM) nature of the materials, originating from band inversion similar to Na_3Bi and Cd_3As_2 . Experimental investigation can shed light on these TDSMs. In NaCdP, band inversion occurs between the *s* and p_y orbitals of phosphorus, while in KCdP, it is between the *s* and *p* orbitals of phosphorus, as illustrated in Figures 4(a) and 4(b), respectively.

Now to confirm the topological properties of XCdP in strained states, surface state calculation has been performed. NaCdP has the topological surface state for (001), (100), and (010) at the Γ point near the Fermi level as shown in Figure 5(a), 5(b), and 5(c), respectively and the corresponding Dirac point is represented in Figure 5(d), 5(e) and 5(f), respectively. The presence of surface states in the surface band structure and its Dirac points confirmed that the NaCdP is a topological Dirac semi-metal in the strained state. Similarly, KCdP has the topological surface state for (001) and (010) at the Γ point as shown in Figure 6(a) and 6(b), respectively and the corresponding Fermi arc surface has been shown in Figure 6(c) and 6(d), respectively. The surface band presented in the surface band structure and corresponding Dirac point confirmed the topological Dirac semimetal feature in the strained state of KCdP. Further investigation shows that the DSM properties of these materials are induced by band inversion between the *s*-orbital and *p*-orbital of Phosphorus and the crossing of the bands indicates that these materials belong to type I DSMs similar to Na_3Bi and Cd_3As_2 category.

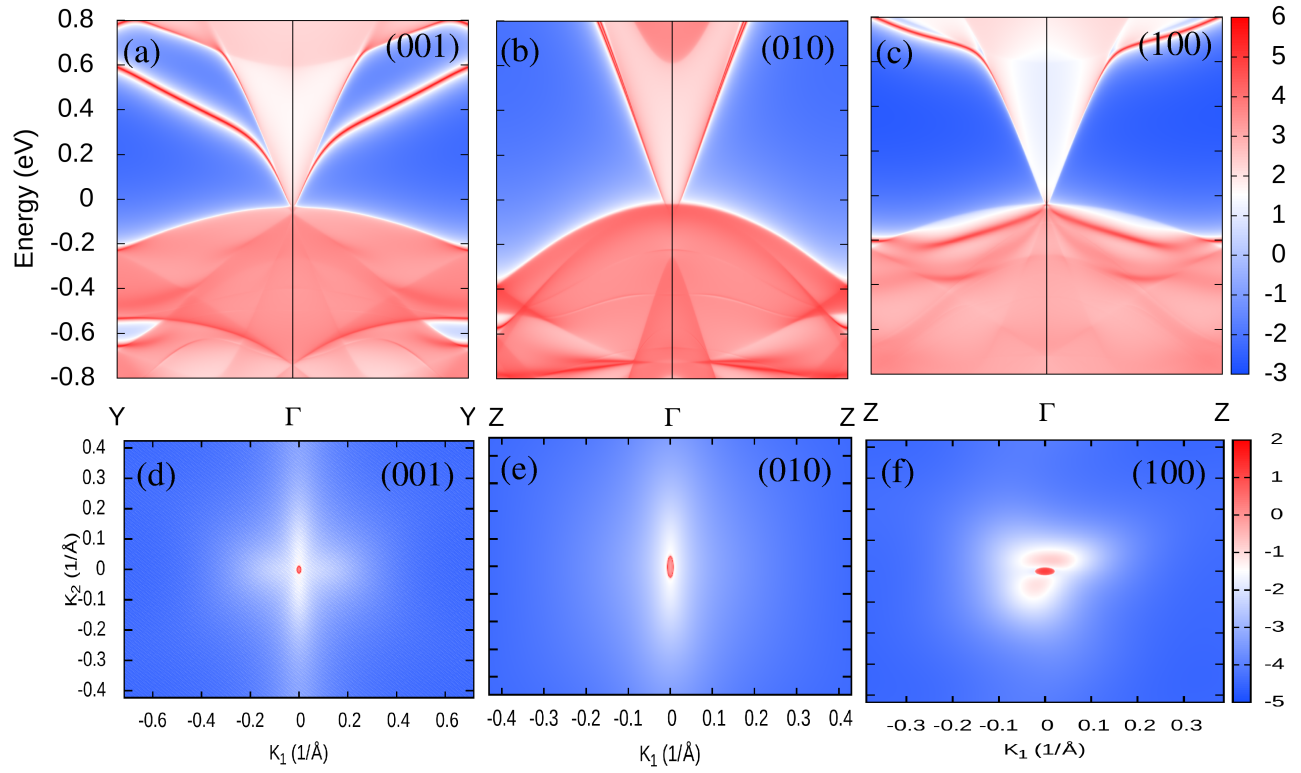


FIG. 5. Surface state of NaCdP (a) (001) plane at $Y-\Gamma-Y$, (b)(010) plane at $Z-\Gamma-Z$ and (c)(100) plane at $Z-\Gamma-Z$. Dirac point at Fermi corresponds to (d) (001) surface, (e)(010) surface and (f)(100) surface.

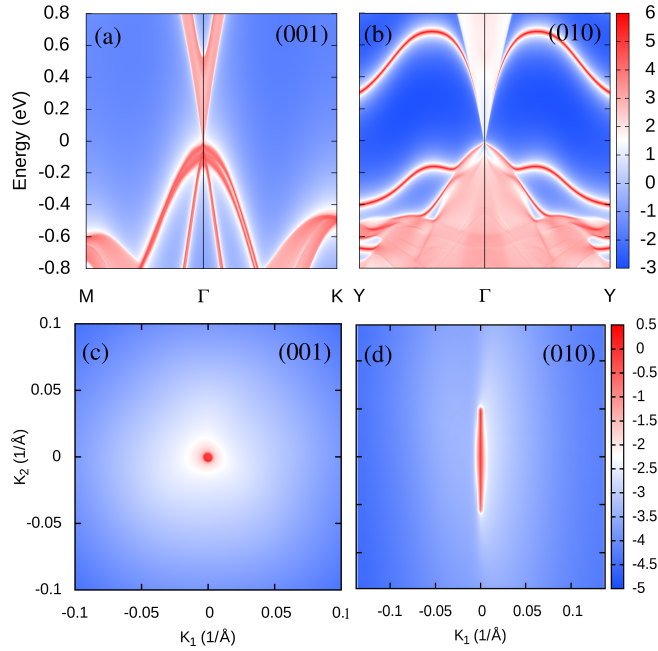


FIG. 6. Surface state of KCdP: (a) (001) plane at $M-\Gamma-K$ and (b)(010) plane at $Y-\Gamma-Y$. Dirac point at Fermi corresponds to (c) (001) surface and (d)(010) surface.

III. COMPUTATIONAL METHODS

Electronic properties of $XCdP$ ($X=Na, K$) compounds have been investigated by the first-principles calculation based on standard density functional theory[35] with the particle potential linearized augmented plane-wave method provided by the VASP package [36]. Generalized gradient approximation (GGA) with Projector augmented wave (PAW)[37] potentials have been utilized to incorporate the exchange-correlation function. The plane-wave basis energy cutoff of 500eV and Γ -centered Monkhorst-pack[38] k-grid of $11 \times 7 \times 6$ for NaCdP and $12 \times 12 \times 6$ for KCdP are used to perform self-consistent calculations (SCF). All the structures, after the application of hydrostatic pressure, were relaxed by employing a conjugate-gradient scheme until the forces on each atom became less than $0.005 \text{ eV}/\text{\AA}$. The band structures were then calculated including SOC using these optimized structures. Maximally localized Wannier functions (MLWF) are used to develop the tight-binding model, which is used to calculate the surface states of the materials using Wannier90 code [39]. WannierTools is used to obtain topological characteristics such as topological surface state, and Fermi surface[40]. A supercell with dimensions of $3 \times 3 \times 2$ has been constructed to calculate the phonon band structure for NaCdP, while a supercell with dimensions of $3 \times 3 \times 1$ has been created for KCdP. The phonon band structures were determined using Density

Functional Perturbation Theory (DFPT), implemented in the phonopy code[41].

IV. CONCLUSION

A series of n-type thermoelectric materials XCdP(X=Na, K) have been investigated by first-principles calculation. The investigation shows that the materials have a finite band gap at ambient pressure. After applying pressure the materials undergo a topological phase transition from normal semiconductors to Dirac semi-metals. In NaCdP the topological phase transition occurs when we apply negative uniaxial pressure on the c-axis, whereas in KCdP the topological phase transition occurs when applying negative tri-axial pressure. The topological Dirac semi-metallic properties in the material have been confirmed by the surface band calculation and

Dirac point present in Fermi arc states. Due to minimal pressure exerted on the current materials, the transition occurs with the crystal structure remaining dynamically stable making these materials ideal for experimental investigations. Further investigation confirms that the DSM properties are induced from the band inversion and these materials are type I DSM in strained states. Our findings may open avenues for additional experimental investigations and technological applications, furthering the ongoing exploration of novel quantum materials.

V. ACKNOWLEDGMENTS

This work is supported by the Science and Engineering Research Board (SERB), Govt. of India, through Grant No. CRG/2022/006419. Author PS would like to thank NPSF C-DAC Pune for providing the HPC facility.

-
- [1] Y. Ren, Z. Qiao, and Q. Niu, “Topological phases in two-dimensional materials: a review,” *Reports on Progress in Physics* **79**, 066501 (2016).
- [2] J. Betancourt, S. Li, X. Dang, J. Burton, E. Tsybal, and J. Velev, “Complex band structure of topological insulator Bi_2Se_3 ,” *Journal of Physics: Condensed Matter* **28**, 395501 (2016).
- [3] S. K. Gupta, A. Kore, S. K. Sen, and P. Singh, “Coexistence of giant rashba splitting, multiple band inversion, and multiple dirac surface states in the three-dimensional topological insulator xSnBi ($\text{x} = \text{rb}, \text{cs}$),” *Physical Review B* **107**, 075143 (2023).
- [4] M. Z. Hasan and C. L. Kane, “Colloquium: topological insulators,” *Reviews of modern physics* **82**, 3045 (2010).
- [5] H. Gao, J. W. Venderbos, Y. Kim, and A. M. Rappe, “Topological semimetals from first principles,” *Annual Review of Materials Research* **49**, 153–183 (2019).
- [6] A. Bernevig, H. Weng, Z. Fang, and X. Dai, “Recent progress in the study of topological semimetals,” *Journal of the Physical Society of Japan* **87**, 041001 (2018).
- [7] H. Huang, J. Liu, D. Vanderbilt, and W. Duan, “Topological nodal-line semimetals in alkaline-earth stannides, germanides, and silicides,” *Physical Review B* **93**, 201114 (2016).
- [8] W. Hou, J. Liu, X. Zuo, J. Xu, X. Zhang, D. Liu, M. Zhao, Z.-G. Zhu, H.-G. Luo, and W. Zhao, “Prediction of crossing nodal-lines and large intrinsic spin hall conductivity in topological dirac semimetal Ta_3As family,” *npj Computational Materials* **7**, 37 (2021).
- [9] T. Liang, Q. Gibson, M. N. Ali, M. Liu, R. Cava, and N. Ong, “Ultrahigh mobility and giant magnetoresistance in the dirac semimetal Cd_3As_2 ,” *Nature materials* **14**, 280–284 (2015).
- [10] Z. Liu, J. Jiang, B. Zhou, Z. Wang, Y. Zhang, H. Weng, D. Prabhakaran, S. K. Mo, H. Peng, P. Dudin, *et al.*, “A stable three-dimensional topological dirac semimetal Cd_3As_2 ,” *Nature materials* **13**, 677–681 (2014).
- [11] S. M. Young and C. L. Kane, “Dirac semimetals in two dimensions,” *Physical review letters* **115**, 126803 (2015).
- [12] B.-J. Yang and N. Nagaosa, “Classification of stable three-dimensional dirac semimetals with nontrivial topology,” *Nature communications* **5**, 4898 (2014).
- [13] B. Peng, C. Yue, H. Zhang, Z. Fang, and H. Weng, “Predicting dirac semimetals based on sodium ternary compounds,” *npj Computational Materials* **4**, 68 (2018).
- [14] S. M. Young, S. Zaheer, J. C. Teo, C. L. Kane, E. J. Mele, and A. M. Rappe, “Dirac semimetal in three dimensions,” *Physical review letters* **108**, 140405 (2012).
- [15] Z. Wang, H. Weng, Q. Wu, X. Dai, and Z. Fang, “Three-dimensional dirac semimetal and quantum transport in Cd_3As_2 ,” *Physical Review B* **88**, 125427 (2013).
- [16] Z. Liu, B. Zhou, Y. Zhang, Z. Wang, H. Weng, D. Prabhakaran, S.-K. Mo, Z. Shen, Z. Fang, X. Dai, *et al.*, “Discovery of a three-dimensional topological dirac semimetal, Na_3Bi ,” *Science* **343**, 864–867 (2014).
- [17] A. Shende, S. K. Gupta, D. Kale, and P. Singh, “First-principles prediction of topological dirac semimetallic phase in NaHgX ($\text{x} = \text{as}$ and bi),” *Physics Letters A* **480**, 128937 (2023).
- [18] H. Huang, S. Zhou, and W. Duan, “Type-ii dirac fermions in the PtSe_2 class of transition metal dichalcogenides,” *Physical Review B* **94**, 121117 (2016).
- [19] C. Le, S. Qin, X. Wu, X. Dai, P. Fu, C. Fang, and J. Hu, “Three-dimensional topological critical dirac semimetal in a MgBi ($\text{a} = \text{k}, \text{rb}, \text{cs}$),” *Physical Review B* **96**, 115121 (2017).
- [20] T.-R. Chang, S.-Y. Xu, D. S. Sanchez, W.-F. Tsai, S.-M. Huang, G. Chang, C.-H. Hsu, G. Bian, I. Belopolski, Z.-M. Yu, *et al.*, “Type-ii symmetry-protected topological dirac semimetals,” *Physical review letters* **119**, 026404 (2017).
- [21] P.-J. Guo, H.-C. Yang, K. Liu, and Z.-Y. Lu, “Type-ii dirac semimetals in the Yd_2S_n class,” *Physical Review B* **95**, 155112 (2017).
- [22] H. Huang, K.-H. Jin, and F. Liu, “Black-hole horizon in the dirac semimetal Zn_2In ,” *Physical Review B* **98**, 121110 (2018).
- [23] S. Fragkos, P. Tsipas, E. Xenogiannopoulou, Y. Panayiotatos, and A. Dimoulas, “Type-iii dirac fermions in

- hfxzr1- xte2 topological semimetal candidate,” *Journal of Applied Physics* **129** (2021).
- [24] C. Sims, “Analogous black holes in type-iii dirac semimetal $\text{ni}_3\text{in}_2\text{x}_2$ ($\text{x} = \text{s}, \text{se}$),” *Crystals* **13**, 847 (2023).
- [25] M. Khan, M. R. Hossain, and M. L. Ali, “Pressure-induced physical properties in topological semi-metals $\text{mas}_2\text{m} = \text{hf}, \text{ti}$,” *Results in Physics* **52**, 106860 (2023).
- [26] S. Khalid, F. P. Sabino, and A. Janotti, “Topological phase transition in laas under pressure,” *Physical Review B* **98**, 220102 (2018).
- [27] L.-K. Zeng, R. Lou, D.-S. Wu, Q. Xu, P.-J. Guo, L.-Y. Kong, Y.-G. Zhong, J.-Z. Ma, B.-B. Fu, P. Richard, *et al.*, “Compensated semimetal lasb with unsaturated magnetoresistance,” *Physical review letters* **117**, 127204 (2016).
- [28] P. Wadhwa, S. Kumar, A. Shukla, and R. Kumar, “First principles investigation of topological phase in xmr material tmsb under hydrostatic pressure,” *Journal of Physics: Condensed Matter* **31**, 335401 (2019).
- [29] Y. Zhou, P. Lu, Y. Du, X. Zhu, G. Zhang, R. Zhang, D. Shao, X. Chen, X. Wang, M. Tian, *et al.*, “Pressure-induced new topological weyl semimetal phase in taas,” *Physical review letters* **117**, 146402 (2016).
- [30] M. Singh, R. Kumar, and R. K. Bibiyan, “Pressure-induced topological phase transition in xmr material ybas: a first-principles study,” *The European Physical Journal Plus* **137**, 633 (2022).
- [31] S. Khalid and A. Janotti, “Trivial to nontrivial topology transition in rare-earth pnictides with epitaxial strain,” *Physical Review B* **102**, 035151 (2020).
- [32] S. Fragkos, R. Sant, C. Alvarez, E. Golias, J. Marquez-Velasco, P. Tsipas, D. Tsoutsou, S. Aminalragia-Giamini, E. Xenogiannopoulou, H. Okuno, *et al.*, “Topological band crossings in epitaxial strained sn₂te,” *Physical review materials* **3**, 104201 (2019).
- [33] P. Gorai, A. Ganose, A. Faghaninia, A. Jain, and V. Stellanović, “Computational discovery of promising new n-type dopable abx₂ zintl thermoelectric materials,” *Materials Horizons* **7**, 1809–1818 (2020).
- [34] E. Herbert, S. Balibar, and F. Caupin, “Cavitation pressure in water,” *Physical Review E* **74**, 041603 (2006).
- [35] W. Kohn and L. J. Sham, “Self-consistent equations including exchange and correlation effects,” *Physical review* **140**, A1133 (1965).
- [36] J. Hafner, “Ab-initio simulations of materials using vasp: Density-functional theory and beyond,” *Journal of computational chemistry* **29**, 2044–2078 (2008).
- [37] M. Torrent, N. Holzwarth, F. Jollet, D. Harris, N. Lepley, and X. Xu, “Electronic structure packages: Two implementations of the projector augmented wave (paw) formalism,” *Computer Physics Communications* **181**, 1862–1867 (2010).
- [38] H. J. Monkhorst and J. D. Pack, “Special points for brillouin-zone integrations,” *Physical review B* **13**, 5188 (1976).
- [39] A. A. Mostofi, J. R. Yates, Y.-S. Lee, I. Souza, D. Vanderbilt, and N. Marzari, “wannier90: A tool for obtaining maximally-localised wannier functions,” *Computer physics communications* **178**, 685–699 (2008).
- [40] Q. Wu, S. Zhang, H.-F. Song, M. Troyer, and A. A. Soluyanov, “Wanniertools: An open-source software package for novel topological materials,” *Computer Physics Communications* **224**, 405–416 (2018).
- [41] A. Togo and I. Tanaka, “First principles phonon calculations in materials science,” *Scripta Materialia* **108**, 1–5 (2015).